Editors' Suggestion | Featured in Physics

Rhythms from Two Competing Periodic Sources Embedded in an Excitable Medium

Khady Diagne,[1] Thomas M. Bury,[2] Marc W. Deyell,[3] Zachary Laksman,[3] Alvin Shrier,[2] Gil Bub,[2] and Leon Glass[2]
[1]Department of Quantitative Life Sciences, McGill University, 550 Sherbrooke W, Montreal, Quebec, H3A 1E3, Canada
[2]Department of Physiology, McGill University, 3655 Promenade Sir William Osler, Montreal, Quebec H3G 1Y6, Canada
[3]Division of Cardiology and Centre for Cardiovascular Innovation, University of British Columbia, Vancouver, British Columbia V6E 1M7, Canada

(Received 31 March 2022; accepted 23 November 2022; published 11 January 2023)

In an excitable medium, a stimulus generates a wave that propagates in space until it reaches the boundary or collides with another wave and annihilates. We study the dynamics generated by two periodic sources with different frequencies in excitable cardiac tissue culture using optogenetic techniques. The observed rhythms, which can be modeled using cellular automata and studied analytically, show unexpected regularities related to classic results in number theory. We apply the results to identify cardiac arrhythmias in people that are due to a putative mechanism of two competing pacemakers.

DOI: 10.1103/PhysRevLett.130.028401

Many physical systems have periodic sources that emit propagating waves. In linear systems (e.g., sound) the waves superimpose and pass through each other. In contrast, an excitable medium is a nonlinear system in which waves do not superimpose but rather collide and annihilate [1]. Following the passage of a wave, there is a refractory period during which a new wave cannot be initiated. Examples of excitable media include the Belousov-Zhabotinsky chemical reaction [2,3] and cardiac tissue [4,5]. In medicine, a cardiac arrhythmia (i.e., an abnormal cardiac rhythm) has been ascribed to the competition between two spontaneous pacemakers with different frequencies: the normal (sinus) pacemaker located in the right atrium and an abnormal (ectopic) pacemaker located in a ventricle that typically has a longer period than the sinus pacemaker [6]. This rhythm is called *parasystole* [6,7]. Earlier work [8,9] showed the analysis of the dynamics in this case is related to a classic problem in number theory and symbolic dynamics [10–12]. However, it did not analyze the spatiotemporal patterns resulting from the two competing independent pacemakers with different frequencies.

In this Letter, we describe the dynamics observed from two periodic sources embedded in an excitable medium. We perform experiments using optogenetic techniques in cardiac tissue [13] with two pacemakers stimulated at different frequencies, and analyze a mathematical model for this system. We apply the results to screen electrocardiographic recordings for cardiac arrhythmias that we postulate are generated by two independent pacemaking sites. The correspondence between dynamics in the clinical and model systems suggests that arrhythmic mechanisms may be identified in patients using wearable cardiac recorders.

We prepared 11 mm diameter monolayers of cardiac cells from neonatal mouse ventricles and genetically modified them to express the light sensitive channel channelrhodopsin-2. Experiments were carried out in a stage top CO_2 incubator at 33–55 °C using optical stimulation and dye-free motion detection as described in Ref. [13]. The monolayers were stimulated at two regions using circular pulses of blue light (~0.018 cm^2) of 100 ms in duration. The first pacemaker, at location N represents the normal sinus pacemaker and is stimulated at a period of T_N. The second, at location V, which is approximately 8.5 mm from N, represents the ventricular ectopic pacemaker and is stimulated with period T_V where $T_V > T_N$. (See the Supplemental Material [14] for a movie.) To track dynamics in the monolayer, we monitored 30 overlapping

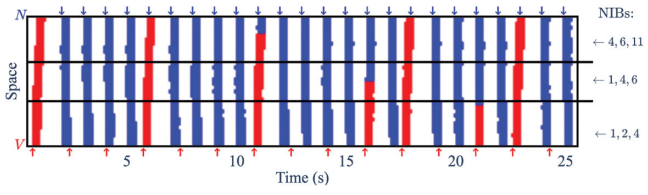

FIG. 1. Space-time plot of an experimental monolayer, which is periodically stimulated with period $T_N = 1.00$ s at N (blue arrows) and $T_V = 1.69$ s at V (red arrows). Waves coming from N are in blue, and those coming from V are in red. The numbers on the right are the number of intervening N beats predicted in a given region of the monolayer. These data are shown at specific locations in Figs. 2(a) and 2(c).

regions of interest (~0.002 cm^2) between N and V. The direction of wave propagation can be observed from a space-time plot as shown in Fig. 1. Not every V beat depolarizes the entire monolayer and collision points with the N beat vary. As such, the sequence of beats varies as a function of space. We describe the sequence of beats by the number of intervening N beats (NIB) between consecutive V beats. At a given point in space, there are 3 unique NIB values that can occur. These values fall into regions, denoted with black horizontal lines in Fig. 1.

To illustrate the rhythms at a given point in space, we generate dot plots showing the interbeat intervals (IBIs). Each IBI is labeled either NN if the interval represents two consecutive N beats, NV for an N beat followed by a V beat, or VN for a V beat followed by an N beat. We define the normalized V cycle length $R = T_V/T_N$ and set the effective refractory period θ as the shortest coupling interval (NV) that generates a wave following an optogenetic stimulus. We ran a total of 30 trials in a total of 7 different monolayers for varying values of T_N and T_V (see Supplemental Material [14]).

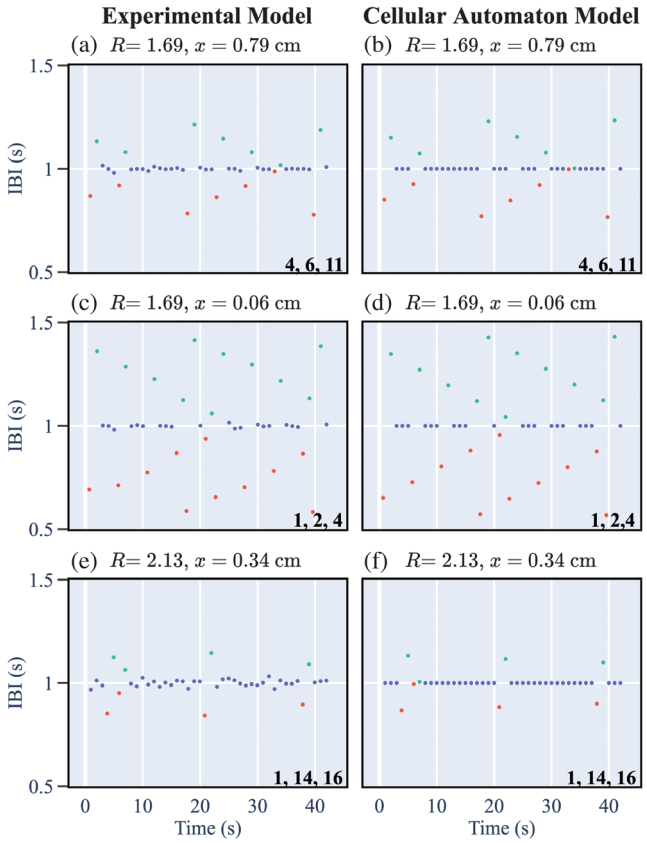

FIG. 2. Interbeat interval plots for the experimental (left) and cellular automaton (right) models at a specific location (x). The dots represent IBIs of type NN (blue), NV (red), and VN (green), where the two letters denote the type of beat at the start and end of the interval. Inset text gives NIBs observed. (a)–(b) 0.79 cm from V at $R = 1.69$ (c)–(d) 0.06 cm from V at $R = 1.69$. (e)–(f) 0.34 cm from V at $R = 2.13$.

The monolayer in Fig. 1 has an effective refractory period of $\theta = 0.54$ s and an average conduction velocity $v = 7.44$ cm/s. Panels (a) and (c) of Fig. 2 show IBIs from this monolayer at different locations (x). Figures 2(a) and 2(c) are from a 60 s trial with $R = 1.69$, showing positions far from ($x = 0.79$ cm) and near to ($x = 0.06$ cm) the V pacemaker. Figure 2(e) is from a 58 s trial in another monolayer ($\theta = 0.68$, $v = 4.28$ cm/s) with slower pacing of the V pacemaker ($R = 2.13$). The NIBs may be obtained by counting the number of dots in between consecutive red dots, and are denoted in the bottom-right corner of each plot.

To model this system, we construct a one-dimensional cellular automaton model [1,15,16]. The cellular automaton consists of a line of excitable cells, with periodic stimulation at both ends. At each time step, an excited cell activates a neighboring cell in a resting state but not a neighboring refractory cell. In Figs. 2(b) and 2(d), we use a time step of 1 ms and a line of 115 cells. Consequently, it takes a wave 114 ms to travel from one pacemaker to the other, which is approximately as observed in experiments in Figs. 2(a) and 2(c). Similarly, we use biophysical parameters obtained in the monolayer in Fig. 2(e) as simulation parameters in the cellular automaton in Fig. 2(f). The IBIs and NIBs for the cellular automaton are plotted in the right panels of Fig. 2. The NIBs obtained from the cellular automaton model agree with those obtained in the experiments.

The mathematical analysis of this system has roots in symbolic dynamics [11,12], number theory [10], and forced oscillators [17,18]. In all these settings, one is interested in the interaction of two oscillations with incommensurate frequencies. A statement of the problem goes back at least to Hedlund [12] who considered the following situation (where we take the liberty to change notation). Assume the unit interval is subdivided into two parts A for $[0, \alpha)$ and B for $[\alpha, 1)$. Now consider the sequence $n\xi \pmod 1$, $-\infty < n < \infty$ where $\xi > 1$ is irrational. A symbolic sequence can be generated by designating the symbol a every time the iterate falls in interval A and b every time the iterate falls in interval B. Hedlund considered the properties of the symbolic sequence [12], Slater showed that between two occurrences of b there could only be 3 different numbers of iterates [10], and Allen and Bélair computed the allowed triplets and applied the result to determine phase locking zones for a simple model of a sawtooth oscillator perturbed by a periodic delta function stimulus [17,18]. Our earlier work applied these methods to parasystole [8], but neglected completely the spatial aspects of propagation. A review with additional references to areas in physics and mathematics connected to this problem is in [11].

We give a brief summary of earlier results ignoring spatial effects [8,9], and then extend this to the spatiotemporal problem relevant here. Let T_N be the unit of time and R, the normalized T_V, be irrational. Starting at an initial time t_0 and phase ϕ_0, times and phases of the jth V beat are given by

$$t_j = F^j(t_0) = t_0 + jR, \tag{1}$$

$$\phi_j = t_j (\mathrm{mod}\ 1) = f^j(\phi_0) = \phi_0 + jR (\mathrm{mod}\ 1), \tag{2}$$

where $j \in \mathbb{N}$ represent the number of V cycles elapsed. It follows that

$$f^j(\phi_0) = F^j(\phi_0) - A_j, \tag{3}$$

where $A_j \in \mathbb{N}$ correspond to the number of N cycles elapsed.

The normalized refractory period is $\alpha = \theta/T_N$. Therefore, V beats that fall in the interval $(0, \alpha)$ are blocked and V beats that fall in the interval $[\alpha, 1]$ are expressed. We are interested in the number of N cycles that occur in between two expressed V beats, the NIBs. Consider an expressed V beat at phase $\phi_0 \in [\alpha, 1]$. What is the minimum number of N cycles $A_k \in \mathbb{N}$, such that $f^k(\phi_0) = (F^k(\phi_0) - A_k) \in [\alpha, 1]$? It turns out there are exactly three possible values for A_k given any $\phi_0 \in [\alpha, 1]$, A_m, A_n and $A_p = A_m + A_n$ (see Supplemental Material [14]). Both in the experimental model of parasystole and parasystole in the human heart, following a V beat the next N beat is blocked. In the heart, this blocking occurs between the atria and the ventricles due to refractory tissue. In the experiment the blocking occurs due to collision of the next N beat with the V beat, or blocking of the N beat at source. Consequently, the NIBs are

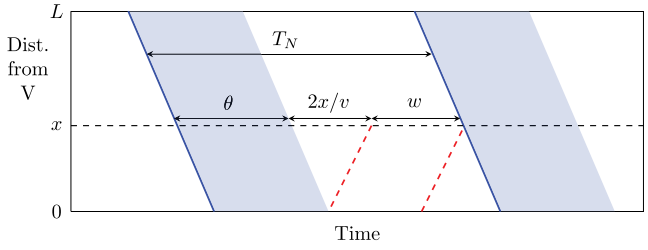

FIG. 3. Space-time schematic illustrating the window $w(x)$ where V beats may occur at a distance x from the V pacemaker. Red dashed lines show the earliest and latest V waves that may arrive at position x. Solid blue lines show wavefronts of N waves. The refractory period (θ) is shaded blue. Full propagation of the second N wave is for illustrative purposes only—a V wave could annihilate the N wave, or block it at the source.

$$A'_m = A_m - 1, \qquad A'_n = A_n - 1,$$
$$A'_p = A_p - 1 = A'_m + A'_n + 1.$$

We now extend the framework to two pacemakers (N and V) separated in space by a distance L [Fig. 3]. We denote x as the distance from the V pacemaker and consider the domain $x \in [0, L]$. Waves are emitted from each pacemaker at a fixed frequency, and travel through space at a constant velocity v. Figure 3 illustrates how at a given point in space (x), there is an interval immediately following an N wave (blue, solid) during which a V wave cannot occur. This interval is made up of the refractory period of the N wave (θ), and the time taken for a wave to propagate from x to the V pacemaker and back again ($2x/v$). The remaining time before the next N wave is the window

$$w(x) = T_N - \theta - 2x/v, \tag{4}$$

which is the time interval between consecutive N waves during which a V wave can occur. For $\theta + 2x/v > T_N$, the window ceases to exist, and we are in a region where no V waves can occur.

We can determine the NIB values as a function of space by reframing the dynamics at a single location (x) into the model considered earlier [8]. At x, the range of phases during which a V beat cannot occur can be written $(0, \alpha(x))$, where

$$\alpha(x) = \frac{1}{T_N}\left(\theta + \frac{2x}{v}\right). \tag{5}$$

This has equivalent NIB values to the dimensionless model, except now α is a function of space. Therefore at different points in space we will observe different NIB triplets, with the region $\alpha(x) > 1$ (if it exists) showing no V waves (infinite NIB). The NIB values as a function of R and $\alpha(x)$ are portrayed in Fig. 4(a). Taking infinite velocity recovers the earlier, dimensionless model of parasystole [8].

Given values for T_N, T_V, θ, x, and V, the three NIB values may be predicted by computing R and α and using the construction in Fig. 4(a). The red crosses mark the R and α values for the experiments and cellular automaton simulations in Fig. 2, showing agreement between predicted NIBs and observation in experiments. The probability of each NIB value at fixed R and α may also be derived analytically (see Supplemental Material [14]). In Fig. 4(b), we plot the NIB probability against $\alpha(x)$ from five runs with $R = 1.69$.

The cardiac arrhythmia parasystole results from an interaction of two pacemakers [6,7] and the above results can be directly applied. We have screened a dataset of electrocardiogram data from 47 patients who experienced frequent ventricular ectopic beats [19]. For each patient, we computed the set of NIB values in each 1-min interval of the recording. Among the sets with three NIB values, if the

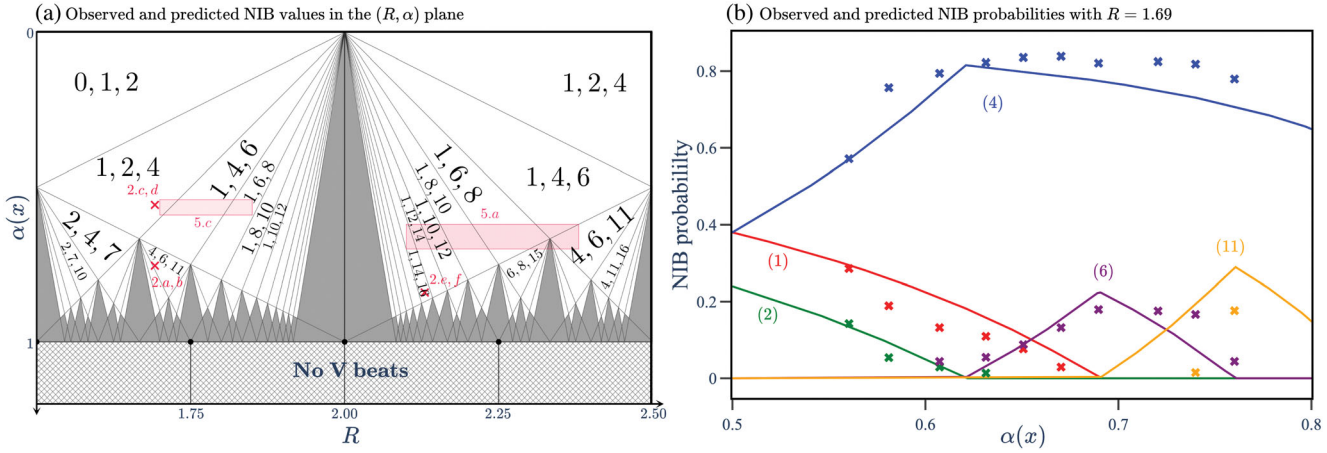

FIG. 4. (a) Allowed values for the number of intervening N beats (NIB) between V beats in the (R, α) plane, where $R = T_V/T_N$ and α is defined in Eq. (5). Shaded areas can be continually divided into smaller regions and their NIBs determined [8]. The cross-hatched region $\alpha \geq 1$ is the range of parameters for which no V beats occur. Red crosses indicate parameter values used in experiments and cellular automaton simulations and red rectangles show parameters observed in the clinical record. In the experimental model and the cellular automaton, (R, α) values are (1.69,0.75), (1.69,0.56), and (2.13,0.84), for Figs. 2(a)–2(f). In the clinical record, (R, α) ranges are given in Fig. 5. (b) Observed and predicted NIBs in space with $R = 1.69$. Continuous lines represent theoretical NIB probabilities. Cross mark symbols represent NIB probabilities across selected experimental monolayers where $R = 1.69$. The NIB values 1, 2, 4, 6, and 11 are labeled in red, green, blue, purple, and orange, respectively.

most commonly occurring set corresponded to one of the NIB triplets shown in Fig. 4(a), the patient was flagged as having a possible parasystole mechanism. Out of the 47 patients, 8 were identified using this method. We show extracts from one of these patients in Figs. 5(a) and 5(c). Clinical details for this patient are available in the

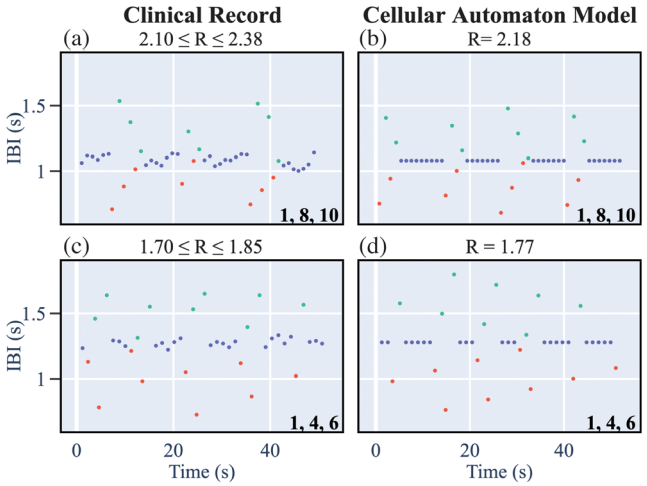

FIG. 5. Interbeat interval plots for a clinical record hypothesized to show a pure parasystole mechanism (left) and the cellular automaton model (right). Inset text gives NIB values observed. (a) Section of clinical record where R and α fluctuate in the range 2.10–2.38 and 0.62–0.70, respectively. (b) Cellular automaton simulation with $T_N = 1.08$, $T_V = 2.35$, $\theta = 0.68$ s, and $x = 0$. (c) Section of clinical record where R and α fluctuate in the range 1.70–1.85 and 0.54–0.59, respectively. (d) Simulation with $T_N = 1.28$, $T_V = 2.26$, $\theta = 0.72$ s, and $x = 0$.

Supplemental Material [14]. For each extract we may obtain a range for T_N from the NN intervals, an approximation for T_V using the average time between V beats where NIB = 1, and an approximation for θ using the minimum coupling interval NV observed in the record for these values of T_N. We estimate $1.00\ \text{s} < T_N < 1.14$, $T_V \approx 2.38$, and $\theta \approx 0.70$ s in panel (a) and $1.22\ \text{s} < T_N < 1.34$, $T_V \approx 2.26$, and $\theta \approx 0.72$ s in panel (b). Since we do not have information on the spatial aspects of the patient's heart, we take $x = 0$, which gives the pattern of beats that occur at the ectopic pacemaker. These lead to a range of R and α values, shown in red in Fig. 4(a). These extracts agree with theoretical predictions [Fig. 4(a)] and cellular automaton simulations [Figs. 5(b) and 5(d)].

There are limitations in the data collected for the current study. In carrying out some of the runs there were complicating factors including the appearance of spontaneous pacemakers that could send off waves interfering with the periodic forcing, initiation of reentrant rhythms, and variable velocity in the dish due to heterogeneity in the tissue culture. Although each of these is worthy of study, as proof of principle in the current Letter, we focus on 5 trials in 2 preparations in which these complicating factors were minimal. In the clinical data, we record fluctuations in pacemaker frequency, but variations in refractory times and conduction velocities are not measured. In addition, resetting of the V pacemaker may occur in clinical contexts; the resulting rhythm is *modulated* parasystole [20,21].

This Letter presents a simple physical model: two periodic sources with incommensurate periods on opposite ends of a linear excitable medium. We compute properties of the sequence of waves from each source at each point in

the medium. We have created an experimental model of this system by periodically stimulating a cardiac sheet and shown that the resulting dynamics agree with the theoretical analysis. These results may have clinical applications: a recent study [22,23] found that large variability in the coupling intervals between sinus and ectopic beats (the NV interval represented by the red dots in Fig. 5) is associated with heart failure. The rhythms considered in this study necessarily display such variable timing. By searching for and identifying the allowed triplets in Fig. 4(a), we are able to carry out large scale screening of clinical records and identify patients whose arrhythmias are generated by a mechanisms of competing pacemakers (parasytole). Thus, techniques originating from early studies in symbolic dynamics and number theory, may be useful in understanding and treating cardiac arrhythmias in people.

This work was supported by grants from the Canadian Institute of Health Research (CIHR) to A. S. (PJT-169008), and the Heart and Stroke Foundation of Canada (RGPIN-2018-05346) and Natural Sciences and Engineering Research Council (NSERC) to G. B. (G-18-0022123). We thank Pierre Fecteau (Icentia) and George Alexander (University of British Columbia) for technical assistance. This research was enabled, in part, by cloud services and support provided by Calcul Québec and Compute Canada.

[1] M. Gerhardt, H. Schuster, and J. J. Tyson, A cellular automation model of excitable media including curvature and dispersion, Science **247**, 1563 (1990).
[2] I. R. Epstein and K. Showalter, Nonlinear chemical dynamics: Oscillations, patterns, and chaos, J. Phys. Chem. **100**, 13132 (1996).
[3] T. R. Chigwada, P. Parmananda, and K. Showalter, Resonance Pacemakers in Excitable Media, Phys. Rev. Lett. **96**, 244101 (2006).
[4] W.-J. Rappel, F. Fenton, and A. Karma, Spatiotemporal Control of Wave Instabilities in Cardiac Tissue, Phys. Rev. Lett. **83**, 456 (1999).
[5] Y. Nagai, H. González, A. Shrier, and L. Glass, Paroxysmal Starting and Stopping of Circulating Waves in Excitable Media, Phys. Rev. Lett. **84**, 4248 (2000).
[6] L. Schamroth, *The Disorders of the Cardiac Rhythm, Second Ed.* (Blackwell, Oxford, UK, 1980).
[7] G. M. Marcus, Evaluation and management of premature ventricular complexes, Circulation **141**, 1404 (2020).
[8] L. Glass, A. Goldberger, and J. Bélair, Dynamics of pure parasystole, Am. J. Physiol. **251**, H841 (1986).
[9] M. Courtemanche, L. Glass, J. Bélair, D. Scagliotti, and D. Gordon, A circle map in a human heart, Physica (Amsterdam) **40D**, 299 (1989).
[10] N. B. Slater, Gaps and steps for the sequence nθ mod 1, Math. Proc. Cambridge Philos. Soc. **63**, 1115 (1967).
[11] R. M. Siegel, C. Tresser, and G. Zettler, A decoding problem in dynamics and in number theory, Chaos **2**, 473 (1992).
[12] G. A. Hedlund, Sturmian minimal sets, Am. J. Math. **66**, 605 (1944).
[13] R. A. Burton, A. Klimas, C. M. Ambrosi, J. Tomek, A. Corbett, E. Entcheva, and G. Bub, Optical control of excitation waves in cardiac tissue, Nat. Photonics **9**, 813 (2015).
[14] See Supplemental Material at http://link.aps.org/supplemental/10.1103/PhysRevLett.130.028401 for additional background, methods, and results.
[15] J. M. Greenberg and S. P. Hastings, Spatial patterns for discrete models of diffusion in excitable media, SIAM J. Appl. Math. **34**, 515 (1978).
[16] G. Bub, A. Shrier, and L. Glass, Spiral Wave Generation in Heterogeneous Excitable Media, Phys. Rev. Lett. **88**, 058101 (2002).
[17] J. Bélair, Periodic pulsatile stimulation of a nonlinear oscillator, J. Math. Biol. **24**, 217 (1986).
[18] T. Allen, On the arithmetic of phase locking: Coupled neurons as a lattice on R^2, Physica (Amsterdam) **6D**, 305 (1983).
[19] T. Bury, C. Lerma, G. Bub, Z. Laksman, M. Deyell, and L. Glass, Long ECGs reveal rich and robust dynamical regimes in patients with frequent ectopy, Chaos **30**, 113127 (2020).
[20] G. Moe, J. Jalife, W. Mueller, and B. Moe, A mathematical model of parasystole and its application to clinical arrhythmias., Circulation **56**, 968 (1977).
[21] V. Schulte-Frohlinde, Y. Ashkenazy, P. C. Ivanov, L. Glass, A. L. Goldberger, and H. E. Stanley, Noise Effects on the Complex Patterns of Abnormal Heartbeats, Phys. Rev. Lett. **87**, 068104 (2001).
[22] W. B. Limpitikul, T. A. Dewland, E. Vittinghoff, E. Soliman, G. Nah, C. Fang, D. S. Siscovick, B. M. Psaty, N. Sotoodehnia, S. Heckbert, P. K. Stein, J. Gottdiener, X. Hu, R. Hempfling, and G. M. Marcus, Premature ventricular complexes and development of heart failure in a community-based population, Heart **108**, 105 (2022).
[23] M. W. Deyell and N. M. Hawkins, Odd couple: Premature ventricular contractions and heart failure, Heart **108**, 86 (2022).